Interaction of SMKT, a killer toxin produced byPichia farinosa, with the yeast cell membranes

ARTICLE *in* YEAST · DECEMBER 2001

Impact Factor: 1.63 · DOI: 10.1002/yea.791 · Source: PubMed

Yeast
Yeast 2001; **18**: 1471–1478.
DOI: 10.1002/yea.791

Research Article

Interaction of SMKT, a killer toxin produced by *Pichia farinosa*, with the yeast cell membranes

Chise Suzuki[1]*, Yoshiji Ando[2] and Sachiko Machida[1]

[1] *National Food Research Institute, 2-1-12 Kannondai, Tsukuba, Ibaraki 305-8642, Japan*
[2] *National Agricultural Research Organization, National Institute of Animal Health, 3-1-5 Kannondai, Tsukuba, Ibaraki 305-0856, Japan*

**Correspondence to:*
C. Suzuki, National Food Research Institute, 2-1-12 Kannon-dai, Tsukuba-shi, Ibaraki-ken 305-8642, Japan.
E-mail: csuzuki@nfri.affrc.go.jp

Received: 30 June 2001
Accepted: 5 July 2001

Abstract

SMKT (salt-mediated killer toxin), a killer toxin produced by the halotolerant yeast, *Pichia farinosa*, kills yeasts of several genera, including *Saccharomyces cerevisiae*. To elucidate the killing mechanism of SMKT, we examined the interaction of SMKT with membranes using liposomes. Leakage of calcein from calcein-entrapped liposomes was observed in the presence of SMKT. Destruction of liposomes was observed by dark-field microscopy. Comparison of intact *S. cerevisiae* cells with SMKT-treated cells by dark-field microscopy indicated that the spherical cell membrane is disrupted by SMKT. Using sodium carbonate extraction, we obtained direct evidence for the first time that SMKT is associated with the membrane of sensitive cells. Our results indicate that SMKT kills sensitive *S. cerevisiae* by interacting with the yeast cell membrane. Copyright © 2001 John Wiley & Sons, Ltd.

Keywords: killer toxin; *Pichia farinosa*; liposomes; dark-field microscopy; calcein; sodium carbonate extraction

Introduction

Killer toxins secreted by yeasts are proteinaceous toxins with diverse activities (Gulubev, 1998). These toxins are mostly specific for certain strains of yeasts, and are usually not effective against other organisms. Some killer toxins have been extensively studied (Bussey, 1991; Tipper and Schmitt, 1991) and the receptor molecules on the cell wall (Hutchins and Bussey, 1983; Schmitt and Radler, 1987) and the target molecules on the plasma membrane (Komiyama *et al.*, 1998) have been identified. However, the most important processes, such as the molecular mechanism of internalization of the killer toxins from the cell surface and the mechanism of self-protection, termed 'immunity', remain unknown.

One of these killer toxins, SMKT, is produced by the halotolerant yeast *Pichia farinosa* KK1. This toxin kills yeasts of several genera in the presence of a high concentration of NaCl or sorbitol (Suzuki and Nikkuni, 1989) and is therefore named 'salt-mediated killer toxin' (SMKT). SMKT consists of two distinct subunits, α (63 amino acid residues) and β (77 amino acid residues) that are processed from a preprotoxin encoded by the chromosomal gene *SMK1* (Suzuki and Nikkuni, 1994).

The wild-type strain of *Saccharomyces cerevisiae* is sensitive to SMKT. However, mutant strains that lack the *SPF1* gene encoding the P-type ATPase are highly resistant to both exogenous SMKT (Suzuki and Shimma, 1999) and endogenously expressed *SMK1* product (Suzuki *et al.*, 2000). SMKT interacts with the cell surface of *spf1* disruptants that have defects in the glycosylation process, suggesting that modified cell wall components sequester SMKT away from the target and confer resistance to exogenous SMKT (Suzuki and Shimma, 1999).

The two subunits of SMKT are folded together in a single ellipsoidal domain in the crystal structure (Kashiwagi *et al.*, 1997) and they interact tightly with each other below pH 5. However, the subunits dissociate above pH 5, resulting in aggregation of the α subunit and concomitant loss of the toxic activity. Circular dichroism (CD) analysis has shown that the soluble β subunit loses its secondary

structure after dissociation from the α subunit (Suzuki *et al.*, 1997).

With regard to the crystal structure, the topology of SMKT is identical to that of the fungal killer toxin KP4 produced by *Ustilago maydis*, despite of the lack of sequence similarity between KP4 and SMKT (Kashiwagi *et al.*, 1997). KP4 is likely to act as a Ca^{2+} channel inhibitor (Gu *et al.*, 1995). On the other hand, SMKT is similar to K1 toxin of *S. cerevisiae*, i.e. it has a subunit structure consisting of a hydrophobic α subunit and a hydrophilic β subunit. A recent study reported that the K1 toxin activates the K^+ channel Tok1p (Ahmed *et al.*, 1999), although it is unclear how the K1 toxin with an optimum pH in the range of pH 4.6–4.8 interacts with the channel in the buffer at pH 7. Further studies are required to determine whether Tok1p is the true target of the toxin or whether *de novo* formation of ion channels by the toxin directly perturbs the cell membrane (Martinac *et al.*, 1990).

As a simple model of biomembranes, liposomes are a useful system to elucidate interactions between biological materials and membranes at the molecular level. The use of dark-field microscopy allows us to visualize the intact morphology and dynamic behaviour of individual liposomes in suspension and allows obtaining real-time images (Magariyama *et al.*, 1995; Saitoh *et al.*, 1998). In the present study, we examined the effect of SMKT on the permeability of lipid bilayers to investigate the direct interaction of SMKT with membranes. We then directly observed the effects of SMKT on liposomes and yeast cells under a dark-field microscope. Our results showed that SMKT interacts only with the sensitive cells in a peripheral manner, as demonstrated in sodium carbonate extraction experiments. The mode of action of SMKT will be discussed, taking into account its interaction with the cell membranes.

Materials and methods

Materials

Phosphatidylcholine (PC), phosphatidylserine (PS), phosphatidylglycerol (PG) and cholesterol were purchased from Avanti Polar Lipids (Birmingham, AL) and used directly without further purification. Mastoparan X was purchased from Bachem (Bubendorf, Switzerland). All other chemicals were obtained locally and were of a high analytical grade.

Multilamellar vesicles (MLVs), calcein-entrapped large unilamellar vesicles (LUVs) for dye-release experiments, and small unilamellar vesicles (SUVs) were prepared as described previously (Machida *et al.*, 2000), with the following modification. After evaporation of the solvent, dried lipid film was hydrated with 10 mM phosphate buffer (pH 4.5).

SMKT was prepared as described previously (Suzuki *et al.*, 1997; Suzuki and Nikkuni, 1994).

Strains and media

Saccharomyces cerevisiae H2071 (*MAT***a**, *his3-Δ1, leu2-3, 112, trp1-289, ura3-52*) (Iida *et al.*, 1994) and CS202A (*spf1::LEU2* in H2071 background) (Suzuki and Shimma, 1999) were used as a sensitive strain and a resistant strain, respectively. YPD containing 1 M sorbitol was used for culturing yeast strains before SMKT treatment. The killer assay medium contained 2.1% YM broth (Difco), 1.5 M sorbitol and 25 mM citrate–phosphate buffer (pH 3.5).

Assays

Leakage of calcein from the vesicles was monitored fluorometrically using Millipore Cytofluor 2300/2350 (Millipore, Bedford, MA)(excitation at 490 nm and emission at 530 nm), as described previously (Machida *et al.*, 2000).

Dark-field microscopy

Liposomes were examined with a dark-field microscope (Zeiss Axiophot, Germany) at 25°C. In order to observe the effect of SMKT on liposomes, 2 μl diluted MLV solution was placed on a cover slip (18 × 18 mm), which was then mounted on a glass slide. SMKT was introduced between the glass slide and the cover slip by placing a small droplet of 10 μM SMKT solution on the slide at the edge of the cover slip.

Yeast cells in the logarithmic phase of growth (1×10^7/ml) were incubated in the killer assay medium in the presence or absence of 0.1 μM SMKT for 1 h at 30°C. Cells were also treated with 3.7% formaldehyde or heated at 65°C for 10 min in the presence or absence of 1% SDS. Those cells were directly observed under a dark-field microscope (Olympus BX50, Japan) equipped with a digital camera (Fujix HC2500, Japan) or under a phase-contrast microscope (Leica DMLB) with a digital camera (Leica DC200).

Sodium carbonate extraction

Spheroplasts were prepared as described previously (Kawamoto *et al*., 1990) with the following modification. After 2-mercaptoethanol treatment, cells were washed with Solution B containing 0.1 M potassium-phosphate buffer (pH 7.5) and 1.2 M sorbitol and were suspended in Solution B containing 50 μg/ml Zymolyase 100T (Seikagaku Co., Japan). Spheroplasts prepared from logarithmically growing cells (2×10^8) and untreated cells (2×10^8) were incubated for 5 min in the killer assay medium containing 1.2 M sorbitol in the presence or absence of 1 μM SMKT. After washing nine times with 1 ml ice-cold citrate–phosphate buffer (pH 3.5) containing 1.2 M sorbitol (CPB/sorb), the cells and spheroplasts were finally washed with 200 μl CPB/sorb, followed by extraction with 200 μl 0.1 M sodium carbonate (SC) (pH 11) containing 1.2 M sorbitol. After 10 min incubation on ice, the SC extracts were separated by centrifugation at $1000 \times g$ for 1 min. After washing once with SC, SC-treated cells were broken with glass beads, as described previously (Suzuki, 1999). SMKT-treated and washed spheroplasts were also broken with glass beads. Lysates of the SC-treated cells and the spheroplasts were centrifuged at $100\,000 \times g$ for 1 h to separate the supernatants (S100) and precipitates (P100). The P100 fractions and the unbroken cell debris were suspended in 50 μl SDS sample buffer (2% SDS, 50 mM Tris–HCl, pH 6.8, 10% glycerol, 2.5% β-mercaptoethanol, 0.1% bromophenol blue). Proteins in the final wash, the SC extracts and the S100 fractions were precipitated in the presence of 12.5% trichloroacetic acid, washed with acetone, and dissolved in 50 μl SDS sample buffer. In the case of SC-treated spheroplasts, the precipitates after SC extraction were suspended in 50 μl SDS sample buffer.

Immunoblotting

Aliquots (10 μl) of samples were analysed by Tricine SDS–PAGE, followed by immunoblotting as described previously, with the following modification (Suzuki, 1999). Protein A-purified rabbit antiserum against the α subunit, that against the β subunit and horseradish peroxidase-linked anti-rabbit immunoglobulin (Bio-Rad Laboratories) were used at dilutions of 1 : 5000, 1 : 1000 and 1 : 3000, respectively. Anti-yeast 3-phosphoglycerate kinase, mouse monoclonal 22C5-D8 (Molecular Probes, Eugene, OR) and horseradish peroxidase-linked anti-mouse immunoglobulin (Bio-Rad Laboratories, Richmond, CA) were used at dilutions of 1 : 10 000 and 1 : 3000, respectively. For detection, the ECL Plus Western Blotting Detection Reagents (Amersham-Pharmacia) were used.

Spheroplast regeneration

Intact cells and spheroplasts were incubated in the presence or absence of SMKT in the killer assay medium containing 1.2 M sorbitol at 30°C for 1 h and diluted in Solution B. In the case of intact cells, cells were appropriately diluted and directly spread on YPD plates. For measurement of the regeneration rate of spheroplasts, 0.1 ml of the appropriate dilution of spheroplasts were mixed with 5 ml YPD containing 1.2 M sorbitol and 3% agarose warmed at 50°C and spread on YPD plates. After 3–5 days incubation, developed colonies were counted.

Results and discussion

Membrane-destabilizing activity

Analysis of killer toxins always involves difficulties associated with assessing the activity in the physiological state, because most killer toxins, including killer toxins of *S. cerevisiae* (Pfeiffer and Radler, 1984) and SMKT (Suzuki and Nikkuni, 1989), have an optimum pH in the acidic range. Considering the habitat of yeasts, as yeasts prefer to grow under acidic conditions, in fruit juice, the finding that killer toxins show optimum activity at acidic pH seems reasonable. The physiological conditions for mammalian cells are not always the same as those for yeasts. Therefore, one should be careful when interpreting the results obtained under conditions that favour the loss of toxin activity. Liposomes prepared under acidic conditions are a powerful tool to overcome these problems. In this study, SUVs, MLVs and calcein-entrapped LUVs were prepared using a buffer at pH 4.5. Such a system allowed us to analyse the interaction between the pH-sensitive killer toxin and the cell membranes.

Figure 1 shows the time course of calcein leakage from LUVs of PC/PG (7 : 3) in the presence of SMKT. Mastoparan-X, a tetradecapeptide toxin from hornet venom, was used as a representative membrane-destabilizing peptide. In the absence of SMKT, no leakage was observed. However, addition of SMKT or mastoparan-X caused rapid release of calcein, although the effect of SMKT

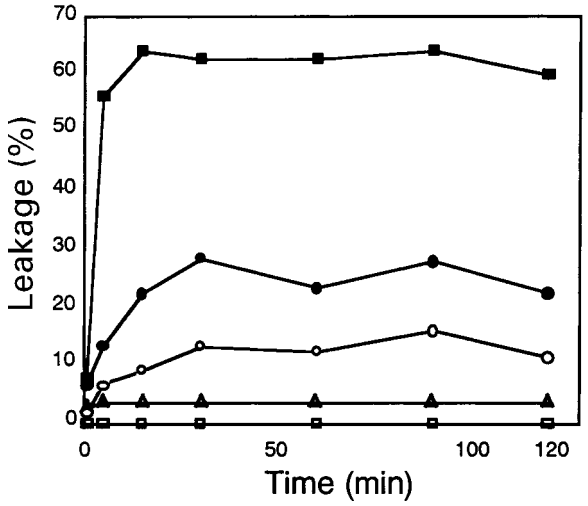

Figure 1. Time course of peptide-induced calcein leakage from acidic LUVs. Dye leakage was monitored fluorometrically (excitation at 490 nm and emission at 530 nm) at 23°C. The fluorescence intensity corresponding to 100% release was determined by the addition of Triton X-100 after 150 min incubation. Samples: closed circles, 5 μM SMKT; open circles, 1 μM SMKT; open triangles, 0.1 μM SMKT; closed squares, 5 μM mastoparan X; open squares, buffer

was less than half that of mastoparan-X. Leakage increased with increasing SMKT concentration. In order to examine the membrane specificity of SMKT, several types of calcein-entrapped LUVs were prepared by changing the ratio of acidic phospholipids and cholesterol. Maximum leakage from LUVs of PC/PS (1 : 1), PC/PS (10 : 1), PC/PS/Chl (10 : 1:1), and PC/PG/Chl (7 : 3:1) in the presence of 5 μM SMKT was 14%, 33%, 28% and 34%, respectively. No significant difference in calcein leakage was observed in these LUVs, suggesting that SMKT non-specifically destabilized the LUVs.

Dark-field microscopy

Spherical liposomes yield a ring-like image because the density of lipids increases at the circumference when a sphere is projected in one plane and where materials with a high refractive index such as lipids distribute in high density yield a bright image by dark-field microscopy (Saitoh *et al.*, 1998).

The process of destruction of liposomes in the presence of SMKT was directly observed under a dark-field microscope. When the buffer was added to the liposome suspension from the edge of the cover slip, a flow of the liposomes was observed. In Figure 2A, a huge MLV is shown at the centre, while running small MLVs appear as light tracks. Under these conditions, no morphological changes were observed. Addition of 5 μM bovine serum albumin to the liposome suspension had no effect (data not shown). On the other hand, when SMKT was added to the liposome suspension, a rapid morphological change was noted. The outer lamella of the huge MLV (Figure 2A) separated off and was divided into small vesicles very rapidly, resulting in aggregation of the small vesicles (Figure 2B). Because SMKT was added from the edge of the cover slip and diffused from there into the liposome

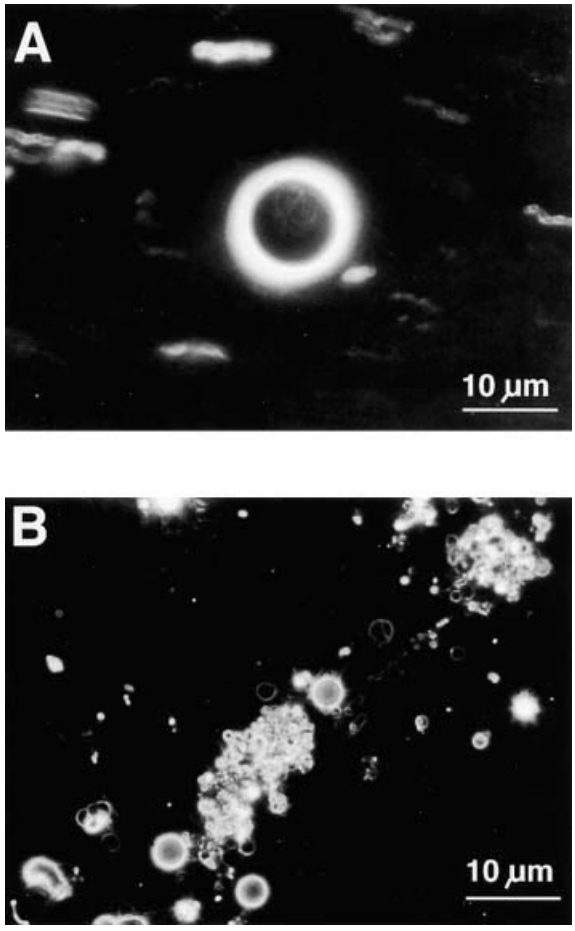

Figure 2. Liposomes observed by dark-field microscopy. (A) Spherical liposomes (MLVs) in the absence of SMKT. A large MLV is at the centre and flowing small vesicles are shown as light tracks. Scale bar = 10 μm. (B) Disrupted liposomes in the presence of SMKT. The large MLV at the centre of panel (A) was disrupted, resulting in small vesicles. No flow was observed at this stage. Scale bar = 10 μm

suspension, the concentration of SMKT was not uniform. Immediate destruction of liposomes was observed in the area near the edge, whereas a relatively slow change in the morphology of the liposomes was observed in the area 5 mm from the edge. These observations are in agreement with the result that the calcein leakage is dependent on the concentration of SMKT (Figure 1). After destruction of the liposomes, no Brownian movement of the liposomes was observed and the liposomes did not flow even when buffer was added, suggesting that these vesicles were stuck to the glass surface.

To exclude the possibility that the interaction between SMKT and the membrane occurs only *in vitro* and does not relate to the killing mechanism, we investigated the effect of SMKT on membranes of yeast cells *in vivo*. The sensitive wild-type cells and resistant *spf1* disruptant cells were treated with SMKT and examined by dark-field microscopy (Figure 3A). In the absence of SMKT, each yeast cell appeared as a ring-like structure with a clear-cut outline, indicating that the yeast cells retained a spherical shape. However, SMKT-treated sensitive cells appeared hazy as a turbid sphere. The outline and inside of the cells could not be distinguished, suggesting that the spherical membrane structure was destroyed by SMKT. The number of cells with a turbid image increased with increasing concentrations of SMKT and prolonged incubation time. Although maximum leakage from LUV was less than 5% in the presence of 0.1 μM SMKT, approximately 60–70% of the sensitive cells showed a turbid image in the presence of 0.1 μM SMKT after 1 h incubation at 30°C. On the other hand, *spf1* disruptants displayed a ring-like image and cells with a turbid image were not observed even in the presence of 1 μM SMKT. These results indicate that there are some sensitivity determinants in the sensitive cells.

To show that the dark-field image of SMKT-treated cells was due to a direct effect of SMKT, the sensitive cells were treated under several conditions and examined by dark-field microscopy (Figure 3B). Cells treated at 65°C for 10 min showed a turbid image similar to SMKT-treated cells. However, cells treated at 65°C for 10 min in the presence of 1% SDS displayed a ring-like image. By this treatment, membrane structures were destroyed and organelles were not visible by phase-contrast microscopy (data not shown). On the other hand, when cells were treated with 3.7% formaldehyde, a standard fixative

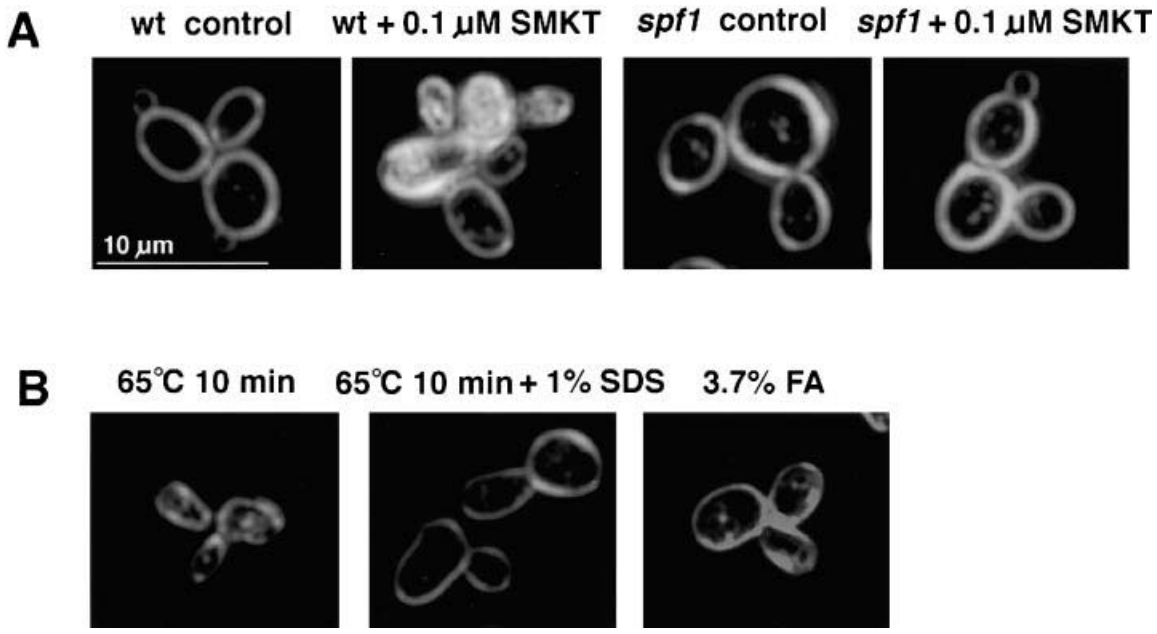

Figure 3. (A) Dark-field images of sensitive (wt) and resistant (*spf1*) strains of *S. cerevisiae* treated with SMKT. Yeast cells were untreated or treated with SMKT (0.1 μM), and observed by dark-field microscopy. Scale bar = 10 μm. (B) Dark-field images of wild-type cells with various treatments. Cells treated at 65°C for 10 min in the presence or absence of 1% SDS and those treated with 3.7% formaldehyde were examined by dark-field microscopy

for observing cell structure, they displayed a ring-like image in dark-field microscopy. These treatments resulted in 100% cell death. These results suggest that the turbid image is due to denaturation and aggregation of cell components and is not necessarily due to cell death. Solubilization of such aggregates by addition of SDS resulted in a ring-like image, although this image may represent an intact cell wall. It is possible that aggregation of membranes and other cellular components may disrupt the spherical structure of the plasma membrane, resulting in eventual cell death.

Interaction of SMKT with the sensitive cells

To investigate how SMKT interacts with yeast cells, we determined the conditions that could effectively strip SMKT from the cells. Experiments were performed using the wild-type strain and the *spf1* disruptant strain. Cells were treated with 1 μM SMKT for 5 min, washed with CPB/sorb until unbound SMKT was not detected in the washing solution. Then cells were treated with 0.1 M SC, which is typically used to extract proteins that are associated with membranes in a peripheral manner (Fujiki *et al.*, 1982). We also analysed SC-extracted SMKT, SMKT binding to cells, and 3-phosphoglycerate kinase (PGK) as a marker of the cytoplasmic proteins (Figure 4A).

Both the α and β subunits were extracted by SC-treatment in the case of wild-type cells. Since PGK was not detected in SC-treated fractions, the results indicated that SC-treatment does not cause cell lysis. This result suggests that SMKT is associated with the cell surface in a peripheral manner. The α subunit was detected in the P100 fraction of the lysates of SC-treated wild-type cells but not in the S100 fraction. When SC-treatment of cells was repeated, more than 90% of SMKT was extracted on the first SC-treatment (data not shown). In this experiment, SC-treated cells were washed with SC again and then broken with glass beads to obtain cell lysates. Therefore, the α subunit in the P100 fraction is not likely to be a contamination from peripherally interacting SMKT and is likely to interact with membranes in a manner different from the SC-extractable α subunit.

Any interaction between SMKT and *spf1* disruptants was detected. Neither the α nor the β subunit was extracted by SC-treatment from *spf1* disruptants and neither was detected in the cell lysates, suggesting that SMKT may be washed out during

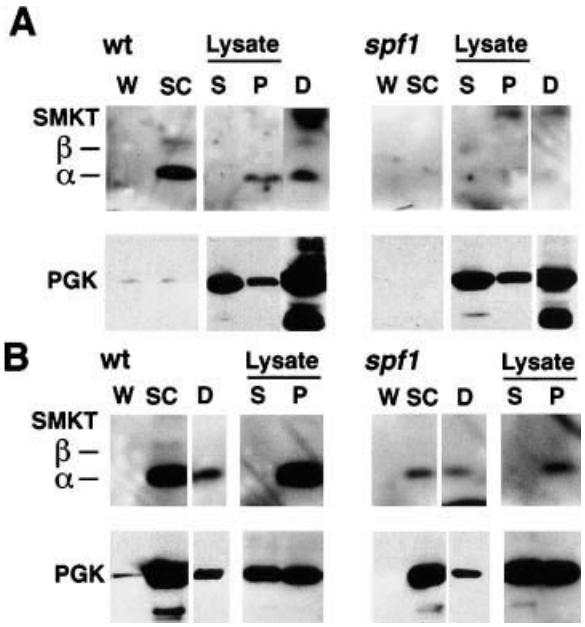

Figure 4. Sodium carbonate (SC) extraction of SMKT-treated cells (A) and spheroplasts (B). (A) The sensitive cells (wt) and resistant cells (*spf1*) were treated with 1 μM SMKT for 5 min and washed 10 times with CPB/sorb. The final washing solution was precipitated by TCA (W). Then cells were treated with 0.1 M SC containing 1.2 M sorbitol (SC). The SC-treated cells were broken with glass beads and the lysates were also centrifuged at 100 000 × *g* for 1 h to separate the S100 fraction (S) and P100 fraction (P). Unbroken cell debris was also analysed (D). The α and β subunits of SMKT and PGK were analysed by immunoblotting. (B) Spheroplasts from the sensitive cells (wt) and resistant cells (*spf1*) were treated with SMKT and then treated with SC as described above. After SC extraction, remaining precipitates were directly dissolved in the SDS sample buffer (D). To examine the internal SMKT, SMKT-treated spheroplasts were broken with glass beads and the lysates were centrifuged at 100 000 × *g* for 1 h to separate the S100 fraction (S) and P100 fraction (P)

the washing process in the case of resistant cells. We have previously indicated that the interaction of SMKT with the surface of *spf1* disruptants was observed only when cells were fixed with formaldehyde just after SMKT treatment (Suzuki and Shimma, 1999). Detection by indirect immunofluorescence microscopy was performed without zymolyase treatment. Under the conditions employed, no intracellular SMKT was detected by mean of fluorescent-labelled IgG because of the barrier function of the cell wall. Therefore, it is reasonable to conclude that SMKT that interacts with the

membrane under the cell wall was not detected in the case of wild-type cells and that only SMKT superficially interacting with the *spf1* disruptants could be detected.

To test whether the cell walls are involved in such interaction, the SC-extraction from SMKT-treated spheroplasts was simultaneously performed (Figure 4B). Both the α and β subunits were extracted by SC from the wild-type spheroplasts as was observed in the wild-type cells. After SC-treatment, very small amount of cell debris was recovered by centrifugation at $1000 \times g$ and PGK was extracted, indicating that SC-treatment destroyed the spheroplasts in spite of the presence of 1.2 M sorbitol. To exclude the possibility that SC-extracted SMKT from the spheroplasts was derived from the inside of the spheroplasts, SMKT-treated spheroplasts were broken with glass beads and the lysates were separated into the S100 fractions and the P100 fractions. Neither the α nor β subunit was detected in the S100 fractions, suggesting that SMKT was associated with spheroplasts of sensitive strain and was extracted by SC, as was observed in wild-type cells.

A small amount of the α subunit was detected in the samples from spheroplasts of the *spf1* strain. This result does not contradict our previous finding that *spf1* disruptants acquire resistance by trapping SMKT on the cell surface (Suzuki and Shimma, 1999). In the absence of the resistant cell walls, SMKT may interact to some extent with the cell membranes of *spf1* disruptants. However, more SMKT was extracted by SC in the case of wild-type spheroplasts, suggesting that SMKT preferably interacts with the membranes of sensitive cells.

To determine the role of the cell wall in the killing activity of SMKT, we next examined the killing effects of SMKT on intact cells and spheroplasts. In the case of intact cells, the viability of the wild-type cells was 3.6% after treatment with 5 μM SMKT for 1 h, whereas that of *spf1* disruptants was 80%. The regeneration rate of the wild-type spheroplasts was 28% in the absence of SMKT and was 1.4% after treatment of 5 μM SMKT for 1 h, suggesting that wild-type spheroplasts are sensitive to SMKT. On the other hand, the regeneration rate of *spf1* spheroplasts was in the range of 2–3% in the presence and absence of SMKT, while less than 5% of unspheroplasted cells remained in the spheroplasts. These results suggest that Spf1p is also involved in the regeneration of spheroplasts. However, it is difficult to conclude that *spf1* spheroplasts are resistant to SMKT when the regeneration rate is less than 5%, because it is impossible to exclude that the regenerated colonies were derived from residual intact cells.

As a simple model of biomembranes, we used liposomes to show that SMKT non-specifically destroys membranes. However, interaction of SMKT with yeast cells was more complicated. Using SC treatment, we obtained for the first time a direct evidence for SMKT interaction with the membrane of sensitive cells. Since SMKT interacts with the membrane of wild-type cells rather than that of *spf1* disruptants, a specific molecule that was synthesized in the presence of Spf1p may involved in the interaction with SMKT. Isolation of the target molecule of SMKT would elucidate not only the killing mechanism but also the function of Spf1p.

Acknowledgements

We thank Dr Y. Magariyama for his support concerning the dark-field microscopy, Drs K. Yoda, Y. Noda and F. Tsuchiya for helpful discussion, and Dr Y. Arata for encouragement. This study was supported in part by a grant-in-aid (Pioneer program) from the Ministry of Agriculture, Forestry and Fisheries, Japan.

References

Ahmed A, Sesti F, Ilan N, Shih TM, Sturley SL, Goldstein SA. 1999. A molecular target for viral killer toxin: TOK1 potassium channels. *Cell* **99**: 283–291.

Bussey H. 1991. K1 killer toxin, a pore-forming protein from yeast. *Mol Microbiol* **5**: 2339–2343.

Fujiki Y, Hubbard AL, Fowler S, Lazarow PB. 1982. Isolation of intracellular membranes by means of sodium carbonate treatment: application to endoplasmic reticulum. *J Cell Biol* **93**: 97–102.

Gu F, Khimani A, Rane SG, Flurkey WH, Bozarth RF, Smith TJ. 1995. Structure and function of a virally encoded fungal toxin from *Ustilago maydis*: a fungal and mammalian Ca^{2+} channel inhibitor. *Structure* **3**: 805–814.

Gulubev WI. 1998. Mycocins (Killer toxins). In *The Yeasts, A Taxonomic Study*, Kurtzman CP, Fell JW (eds). Elsevier: Amsterdam; 55–62.

Hutchins K, Bussey H. 1983. Cell wall receptor for yeast killer toxin: involvement of (1→6)-β-D-glucan. *J Bacteriol* **154**: 161–169.

Iida H, Nakamura H, Ono T, Okumura MS, Anraku Y. 1994. *MID1*, a novel *Saccharomyces cerevisiae* gene encoding a plasma membrane protein, is required for Ca^{2+} influx and mating. *Mol Cell Biol* **14**: 8259–8271.

Kashiwagi T, Kunishima N, Suzuki C, *et al*. 1997. The novel acidophilic structure of the killer toxin from halotolerant yeast demonstrates remarkable folding similarity with a fungal killer toxin. *Structure* **5**: 81–94.

Kawamoto S, Arai N, Kobayashi M, *et al*. 1990. Isolation and characterization of mutants of *Saccharomyces cerevisiae* resistant to killer toxin of *Kluyveromyces lactis*. *J Ferment Bioeng* **70**: 222–227.

Komiyama T, Shirai T, Ohta T, *et al*. 1998. Action properties of HYI killer toxin from *Williopsis saturnus* var. *saturnus*, and antibiotics, aculeacin A and papulacandin B. *Biol Pharm Bull* **21**: 1013–1019.

Machida S, Niimi S, Shi X, Ando Y, Yong Y. 2000. Design of a novel membrane-destabilizing peptide selectively acting on acidic liposomes. *Biosci Biotechnol Biochem* **64**: 985–994.

Magariyama Y, Sugiyama S, Muramoto K, Kawagishi I, Imae Y, Kudo S. 1995. Simultaneous measurement of bacterial flagellar rotation rate and swimming speed. *Biophys J* **69**: 2154–2162.

Martinac B, Zhu H, Kubalski A, *et al*. 1990. Yeast K1 killer toxin forms ion channels in sensitive yeast spheroplasts and in artificial liposomes. *Proc Natl Acad Sci USA* **87**: 6228–6232.

Pfeiffer P, Radler F. 1984. Comparison of the killer toxin of several yeasts and the purification of a toxin of type K2. *Arch Microbiol* **137**: 357–361.

Saitoh A, Takiguchi K, Tanaka Y, Hotani H. 1998. Opening-up of liposomal membranes by talin. *Proc Natl Acad Sci USA* **95**: 1026–1031.

Schmitt M, Radler F. 1987. Mannoprotein of the yeast cell wall as primary receptor for the killer toxin of *Saccharomyces cerevisiae* strain 28. *J Gen Microbiol* **133**: 3347–3354.

Suzuki C. 1999. Secretion of a protoxin post-translationally controlled by NaCl in a halotolerant yeast, *Pichia farinosa*. *Yeast* **15**: 123–131.

Suzuki C, Kashiwagi T, Tsuchiya F, *et al*. 1997. Circular dichroism analysis of the interaction between the α and β subunits in a killer toxin produced by a halotolerant yeast, *Pichia farinosa*. *Protein Engin* **10**: 99–101.

Suzuki C, Kawano M, Kashiwagi T, Arata Y, Kawasumi T, Kashiwagi Y. 2000. Lethal effect of the expression of a killer gene *SMK1* in *Saccharomyces cerevisiae*. *Protein Engng* **13**: 73–76.

Suzuki C, Nikkuni S. 1989. Purification and properties of the killer toxin produced by a halotolerant yeast, *Pichia farinosa*. *Agric Biol Chem* **53**: 2599–2604.

Suzuki C, Nikkuni S. 1994. The primary and subunit structure of a novel type killer toxin produced by a halotolerant yeast, *Pichia farinosa*. *J Biol Chem* **269**: 3041–3046.

Suzuki C, Shimma Y. 1999. P-type ATPase *spf1* mutants show a novel resistant mechanism for the killer toxin SMKT. *Mol Microbiol* **32**: 813–824.

Tipper DJ, Schmitt MJ. 1991. Yeast dsRNA viruses: replication and killer phenotypes. *Mol Microbiol* **5**: 2331–2338.

